Characterizing Excited States of CH_5^+ with Diffusion Monte Carlo†

Charlotte E. Hinkle and Anne B. McCoy*

Department of Chemistry, The Ohio State University, Columbus, Ohio 43210

Received: October 8, 2007; In Final Form: December 14, 2007

The spectroscopy and dynamics of protonated methane have been of long-standing interest due to the unusual and highly fluxional behavior of CH_5^+. This reflects the fact that the ground-state wave function for CH_5^+ has nearly equal amplitude at the 120 equivalent minima and at the saddle points that connect these minima. While low-resolution spectra of CH_5^+ have been assigned, the nature of the couplings between the CH stretches and the low-frequency modes is not as well characterized. An understanding of this will be important in the interpretation of rotationally resolved spectra. In this work, fixed-node diffusion Monte Carlo techniques are used to calculate energies and probability amplitudes for several excited states. The calculated energies are shown to be in good agreement with previously reported vibrational configuration interactions calculations. Analysis of the 12-dimensional probability amplitudes shows that there are strong couplings between the high-frequency CH stretch and HCH bend motions and the low-frequency modes that lead to isomerization CH_5^+.

1. Introduction

Protonated methane is a molecule that has been of long standing interest both experimentally and theoretically. This interest is derived from the expectation that CH_5^+ could be an important species in the chemistry that takes place in dense interstellar clouds,[1] due to the relatively deep CH_4D^+ minimum on the $CH_3^+ + HD \rightarrow CH_2D^+ + H_2$ reactive potential surface. The number of studies on CH_5^+ has increased rapidly over the past several years with two reports of rotationally resolved spectra, first by Oka and co-workers,[2] and, more recently, by Nesbit and co-workers.[3] During the same period of time, a lower-resolution, laser induced reaction (LIR) spectrum of CH_5^+ was reported by Schlemmer and co-workers.[4] The LIR spectrum contains two prominent peaks, a band at 1200 cm^{-1} that has been assigned to HCH bends and a broad band, which extends from 2200 to 3400 cm^{-1}, that has been assigned to a variety of CH stretching motions.[3,4] High-resolution spectra have been recorded for the 2800−3100 cm^{-1} region and reflect excitation of CH stretching fundamentals. While qualitative assignments have been provided for the LIR spectrum, to date the majority of the rotational transitions remain unassigned.[5]

From a theoretical standpoint, CH_5^+ introduces a number of interesting features as well as challenges. Starting with the earliest electronic structure calculations, it was clear that the potential for CH_5^+ contained several low-energy saddle points that appeared to be accessible at the zero-point level.[6,7] The structure of the minimum energy configuration of CH_5^+ and its geometries at the three lowest energy saddle points are shown in Figure 1. The two structures with C_s symmetry can be characterized by a H_2 moiety interacting with the CH_3^+ group. This characterization is based on the observation that the shortest hydrogen/hydrogen distance in these structures is roughly two-thirds the length of the next shortest hydrogen/hydrogen distance. Analysis of the structures of the minima and the two lowest energy saddle points shows that any pair of the 120 minima on the potential can be connected through a series of low-energy saddle points, none of which has an energy that is higher than 350 cm^{-1} when the stationary points are evaluated at the CCSD(T)/aug-cc-pvtz level of theory/basis.[8] More strikingly, when the harmonic zero point energy is added to the electronic energies of the stationary points, the range of energies decreases to less than 30 cm^{-1}.[9]

This observation raises the questions of how one should think about the structure of CH_5^+ and how the fluxionality of CH_5^+ is reflected in the infrared spectrum. Through a series of studies by us and others, using methods including classical trajectory simulations,[10,11] path integral Monte Carlo (PIMD),[12,13] diffusion Monte Carlo (DMC),[14−18] variational approaches[3,19] and analysis of model Hamiltonians,[20] the authors conclude that the ground state of CH_5^+ is delocalized among all 120 equivalent minima on the potential surface as well as the 180 saddle points that connect these minima. In spite of the high level of fluxionality displayed by CH_5^+, molecular dynamics and PIMD simulations run at 300 and 0 K DMC simulations all show that 70−80% of the sampled configuration space corresponds to the molecule having a C_s-like structure, defined by Marx as structures for which the shortest hydrogen/hydrogen distance is smaller than 1.15 Å.[11,12,18] This observation has led to further electronic structure studies of the nature of the bonding in CH_5^+.[21−23]

The question remains as to how this fluxional behavior is reflected in the reported spectra. Interestingly, we found that we could reproduce the LIR spectrum[4] by first evaluating spectra obtained by either harmonic or variational calculations that are based on the normal mode coordinates evaluated at one of the three stationary points on the potential, weighting the three calculated spectra by the relative probability amplitudes at each of these stationary points, and summing the resulting spectra.[3,24] This procedure also gives good agrement with a convolution of the high-resolution spectrum, reported by Nesbitt and co-workers. This is, at first, somewhat surprising, given the large amplitude motions exhibited by the ground state of CH_5^+. On the other hand, difficulties in assigning the high-resolution

† Part of the "William A. Lester, Jr., Festschrift".

* Author to whom correspondence should be addressed. E-mail: mccoy@chemistry.ohio-state.edu.

10.1021/jp709828v CCC: $40.75
Published on Web 02/06/2008

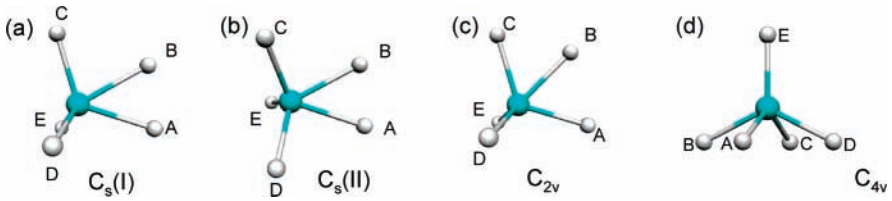

Figure 1. Structures of the four lowest energy stationary points on the CH_5^+ potential surface.[8] The A−E labels are included to help show the relationship among the structures. The minimum energy structure is shown in (a). The (b) C_s(II) saddle point has an energy of 29 cm^{-1} relative to the global minimum. The energies of the (c) C_{2v} and (d) C_{4v} structures are 341 and 1180 cm^{-1} above the global minimum, respectively.

TABLE 1: The CH Bond Lengths at the Four Stationary Points, Depicted in Figure 1[a]

CH bond structure	CH bond length (Å)			
	C_s(I)	C_s(II)	C_{2v}	C_{4v}
CH_A	1.20	1.20	1.14	1.12
CH_B	1.20	1.20	1.16	1.12
CH_C	1.11	1.10	1.14	1.12
CH_D	1.09	1.10	1.09	1.12
CH_E	1.09	1.08	1.09	1.08

[a] All distances are reported in angstroms and are calculated using the CCSD(T) potential of Jin et al.[8]

TABLE 2: The HH Bond Lengths at the Four Stationary Points, Depicted in Figure 1[a]

HH bond structure	HH bond length (Å)			
	C_s(I)	C_s(II)	C_{2v}	C_{4v}
H_AH_B	0.95	0.94	1.18	1.43
H_AH_C	2.04	2.02	2.00	2.02
H_AH_D	1.72	1.55	1.75	1.43
H_AH_E	1.72	1.84	1.75	1.87
H_BH_C	1.44	1.55	1.18	1.43
H_BH_D	1.94	2.02	1.94	2.02
H_BH_E	1.94	1.84	1.94	1.87
H_CH_D	1.79	1.76	1.75	1.43
H_CH_E	1.79	1.85	1.75	1.87
H_DH_E	1.88	1.85	1.81	1.87

[a] All distances are reported in angstroms and are calculated using the CCSD(T) potential of Jin et al.[8]

spectra hint that CH_5^+ is more complicated than this simple treatment would imply.

Based on the success of this earlier work and the apparent strong couplings among various vibrational degrees of freedom, we embarked on a study of the nature of the vibrationally excited states that are accessed in the experimental spectra. This study is based on the application of fixed-node DMC approaches, initially proposed by Anderson,[25,26] in which an excited state is evaluated by requiring that the wave function changes sign at a specified value of the internal coordinates. While, at first glance, this may appear to be a questionable approach to take for a system as fluxional as CH_5^+, we are encouraged by the excellent agreement we previously obtained on several floppy systems, specifically $Ne_2OH(A^2\Sigma^+)$, $Ne_2SH(A^2\Sigma^+)$,[27] $H_3O_2^-$,[28] and $H_5O_2^+$,[29,31] for which direct comparisons to results of variational calculations could be made. Before discussing this approach further, we return to the stationary points of CH_5^+.

2. System

The potential energy surface for CH_5^+ is characterized by 120 equivalent minima, separated by a series of low-energy saddle points. These are depicted in Figure 1 along with the corresponding energies, calculated using a global CCSD(T)/aug-cc-pvtz-based potential surface, developed by Jin et al.[8] While the precise values of the calculated energies of the stationary points depend on the level of electronic structure theory and the basis set that are employed, recent studies are all consistent with the lowest energy structure having C_s symmetry, as is shown in Figure 1a. In this configuration, the shortest hydrogen/hydrogen distance is 65% the value of the second shortest distance. In the discussion that follows, the shortest hydrogen/hydrogen distance is between the hydrogen atoms that are labeled A and B. The second shortest hydrogen/hydrogen distance involves the hydrogen atoms that are labeled B and C. As shown in Figure 1, the remaining hydrogen atoms are labeled D and E and are related by reflection through the plane of symmetry. The values of the CH and HH distances at this stationary point are reported in Tables 1 and 2, respectively. From the distances reported in these tables, one finds that the HCH angles that involve the hydrogen atoms labeled C, D and E are 109.3° and 119.4°. This is consistent with a nearly tetrahedral bonding configuration around the carbon atom and leads us to refer to these four atoms as the CH_3^+ group.

There is a low-lying saddle point with C_s symmetry, shown in Figure 1b. This saddle point has an energy of 29 cm^{-1} above the global minimum.[8] Motion between the C_s(II) saddle point and the C_s(I) minimum corresponds to rotation of the CH_3 group by 30° about the axis that connects the center of mass of the three hydrogen atoms in the CH_3 group and the carbon atom. In the C_s(II) configuration, the hydrogen atoms labeled A and B and those labeled C and D are related by reflection through the plane of symmetry. This symmetry can be seen in the atom/atom distances reported in Tables 1 and 2.

A second low-energy saddle point has C_{2v} symmetry and is shown in Figure 1c. In this case, the saddle point relaxes to the minimum through motion of H_B toward H_A, concurrent with a rocking motion of the H_DCH_E group. In this structure, the CH_B bond lies along the C_2 axis, H_A and H_C lie in one of the reflection planes while H_D and H_E lie in the other reflection plane.

In this study, we also consider a third saddle point that has C_{4v} symmetry, with an energy of 1180 cm^{-1} above the global minimum. Unlike the other saddle points, it is a second-order saddle point with the imaginary frequency modes corresponding to displacement of H_E off the C_4 symmetry axis. As we will show, vibrational excitation can increase the probability amplitude near this configuration. Finally, analysis of the imaginary frequency modes indicates that motion along the minimum energy path, away from this saddle point, leads to the C_s(II) saddle point.

Before continuing to a discussion of the methods used in this study, we need to define the two coordinates that correspond to curvilinear version of the modes with imaginary frequency at the C_s(II) and C_{2v} saddle points. The C_s isomerization coordinate corresponds to motion along $\phi_{\alpha,\beta}$, where α = A or B and β = C, D or E. More precisely, to determine $\phi_{\alpha,\beta}$, we define a body-fixed axis system. Here, the *z*-axis contains the carbon atom and the center of mass of the hydrogen atoms

TABLE 3: The Values of the Three Isomerization Coordinates, Defined in the Text, Evaluated at the Four Stationary Points, Shown in Figure 1[a]

isomerization coordinate	C_s(I)	C_s(II)	C_{2v}	C_{4v}
$\|q\|$	0.49	0.61	0.00	0.00
$\phi_{A,C}$	0	31	0	143
$\phi_{B,C}$	180	149	180	37
$\phi_{A,D}$	118	149	116	37
$\phi_{B,D}$	62	31	64	143
$\phi_{A,E}$	118	90	116	90
$\phi_{B,E}$	62	90	64	90
$\sigma_{C_{4v}}$	20.59	21.64	20.65	0.00

[a] All distances are reported in angstroms, angles in degrees, and are calculated using the CCSD(T) potential of Jin et al.[8]

labeled C, D and E. The H_A-H_B bond lies parallel to the *xz* plane with the molecule oriented so that the *x*-coordinate of H_α is positive. Finally, we define $\phi_{\alpha,\beta}$ as the angle between the CH_β vector and the *xz* plane. The six values for $\phi_{\alpha,\beta}$ at each of the four stationary points shown in Figure 1 are reported in Table 3. The C_{2v} isomerization coordinate is defined as

$$|q| = |r_{H_BH_C} - r_{H_AH_B}| \tag{1}$$

or equivalently, the H_AH_B/H_BH_C asymmetric stretch.

Because we could not find a single coordinate to define motion away from the C_{4v} structure, we determine the extent of C_{4v} character displayed by a particular state by evaluating the probability amplitude as a function of the standard deviation among the four smallest HCH angles, $\sigma_{C_{4v}}$. When the geometry of CH_5^+ is close to the C_{4v} saddle point, $\sigma_{C_{4v}} = 0$. This definition will not discriminate structures near the C_{4v} saddle point and, for example, those with D_{3h} point group symmetry as both have four equal HCH angles. On the other hand, when we plot the probability amplitude as functions of both $\sigma_{C_{4v}}$ and the sum of the four smallest angles or the standard deviation among the values of the six largest HCH angles, we find that the amplitude near $\sigma_{C_{4v}} = 0$ also has the values of these other variables that correspond to the C_{4v} saddle point geometry and not the geometry of the D_{3h} saddle points. The equilibrium values of $|q|$ and $\sigma_{C_{4v}}$ are reported in Table 3.

3. Theory

In the present study we use DMC approaches to evaluate energies, wave functions and probability amplitudes for selected excited states of CH_5^+. The details of DMC[25,26] and our implementatation[9,32] have been presented in detail elsewhere.

In DMC, we evaluate the wave function and energy of the state of interest by employing statistical approaches to obtain the long-time solution to the time-dependent Schrödinger equation in which the time variable, *t*, has been replaced by an imaginary time variable, $\tau = it/\hbar$. For the ground state, we use the global potential surface developed by Bowman and coworkers.[8] In the excited-state calculations, we define a variable, ζ, which is zero at the value of the internal coordinates at which the wave function changes sign. We then perform a pair of simulations to obtain the excited-state energy and wave function. In the first simulation, we use the global potential of Jin et al.[8] when $\zeta < 0$ and make the potential infinite for positive values of ζ. The second simulation uses the global potential for CH_5^+ when $\zeta > 0$ and an infinite potential for negative values of ζ. By introducing the infinite potential we replace each of the excited-state calculations with a pair of ground-state calculations. Because we are performing separate simulations for positive and negative values of ζ, we refer to the resulting wave functions by the sign of ζ. By summing the wave functions obtained from the two separate simulations we obtain the full wave function. The energies associated with the two separate simulations are equal, within statistical uncertainties.

4. Results

4.1. Numerical Details. Diffusion Monte Carlo simulations are performed using a time step, $\Delta\tau$, of 10 a.u. The average value of

$$W(\tau) = \bar{V}(\tau) - \alpha\frac{N(\tau) - N(0)}{N(0)} \tag{2}$$

provides the energy. Here $\alpha = 0.1$ hartree is found to effectively control the number of diffusing particles, or walkers, and consequently the magnitude of the fluctuations of $W(\tau)$.[9] $\bar{V}(\tau)$ represents the average potential energy, and $N(\tau)$ gives the number of walkers at τ. Each simulation is repeated four times using different initial conditions. The reported energies reflect the average of the four simulations. In excited-state calculations, where the functional form of ζ can be determined by symmetry, the wave functions and energies are evaluated for $\zeta > 0$. When the exact functional form of ζ cannot be determined by symmetry, we employ adiabatic diffusion Monte Carlo (ADMC) calculations to determine the functional form of ζ and the energy of the excited state.[32] As we discussed above, this procedure involves making the potential infinite for either positive or negative values of ζ. As the wave function must be zero in regions of configuration space where the potential is infinite, walkers can only exist on one side of the nodal surface. Walkers that cross the nodal surface are removed from the simulation. Even when the walker remains on the same side of the nodal surface, it is possible that, had smaller time steps been employed, the walker would have crossed the nodal surface twice. Following Anderson, the probability that a walker has crossed the nodal surface an even number of times is given by[26]

$$P_{\text{recross}} = e^{-(4x'x''/(2\sigma^2))} \tag{3}$$

where

$$\sigma = \frac{2\Delta\tau}{\mu} \tag{4}$$

In P_{recross}, x' and x'' refer to the positions of the walker at time τ and $\tau + \Delta\tau$, respectively. The mass, μ, is the reduced mass associated with the coordinate used to define the nodal surface. In all cases, the nodal surface is defined as

$$\zeta = \frac{r_{\alpha\beta} \pm r_{\beta\gamma}}{\sqrt{2}} - \delta \tag{5}$$

where δ is a real number, the value of which either is determined to be zero by symmetry or is evaluated in the ADMC simulations. Finally,

$$\frac{1}{\mu} = \frac{1}{m_\alpha} + \frac{1 \pm \cos\theta_{\alpha\beta\gamma}}{m_\beta} \tag{6}$$

where α, β, and γ represent the atoms in CH_5^+ and $m_\gamma = m_\alpha$.

Once energies have been evaluated for the excited states, fixed node calculations are performed in order to obtain probability amplitudes using the descendent weighting procedure.[33] Here the probability amplitude at the position of a given walker is

TABLE 4: The Energies of the Excited States[a]

ζ (Å)	energy (cm^{-1})	VCI energies (cm^{-1})	% C_{4v}[b]
c	44 ± 5		0.07
$(1/\sqrt{2})(r_{H_AH_B} - r_{H_BH_C})$	271 ± 5	175	<0.01
$(1/\sqrt{2})(r_{H_CH_D} - r_{H_CH_E})$	990 ± 5		0.40
$(1/\sqrt{2})(r_{H_BH_D} - r_{H_BH_E})$	1128 ± 5	1116	0.07
$(1/\sqrt{2})(r_{CH_A} - r_{CH_B})$	2432 ± 5	2468	<0.01
$(1/\sqrt{2})(r_{CH_D} - r_{CH_E})$	3023 ± 5	3067	0.23
$(1/\sqrt{2})(r_{CH_A} + r_{CH_C}) - 1.65489$[d]	2974 ± 5		0.09
$(1/\sqrt{2})(r_{CH_D} + r_{CH_E}) - 1.57878$[d]	3144 ± 5	2983	0.06

[a] Energies calculated by fixed-node DMC and are reported relative to the zero point energy (10916 ± 5 cm^{-1}). For comparison, the VCI energies reported in ref 3 are also given. All energies are given in cm^{-1}. [b] % C_{4v} provides a percentage of the probability amplitude for which $\sigma_{C_{4v}} < 2.5°$, $\sigma_{C_{4v}} = 0.06\%$ for the ground state. [c] The node is defined as having two of the HH distances equal. [d] The values of δ in eq 5 reflect the averages of four independent ADMC simulations. The statistical uncertainties in these values are 8×10^{-5} Å for the CH_A/CH_C symmetric stretch and 4×10^{-5} Å for the CH_D/CH_E symmetric stretch.

proportional to the number of descendents after 25 time steps. In order to obtain reliable statistics, this procedure is repeated 25 times and the wave function is propagated for 200 time steps between samplings. In cases, like the CH bond length distribution, where there are five distance distributions, the reported probability distribution reflects the sum of these distributions.

4.2. Excited-State Energies. We calculated the energies and wave functions for several excited states. The equation for ζ along with the energies is reported in Table 4. For comparison, the energies calculated using the vibrational configuration interaction (VCI) approach, as implemented in the program MULTIMODE,[34] are also reported.[3] In all but two cases the value of δ at the node is zero, by symmetry. The exceptions are the CH_A/CH_C and CH_D/CH_E symmetric stretches, where the position of the nodal surface was determined using the ADMC approach.[32]

The two lowest energy states correspond to the fundamentals in the C_s(II) and C_{2v} isomerization coordinates, defined in section 2. Specifically, for the state at 44 cm^{-1}, the nodal surface is defined as two of the HH distances being equal. At first consideration, this may not appear to correspond to putting a node at the C_s(II) saddle point. Analysis of the probability amplitude for this state indicates that this is indeed the case. For this reason, we will refer to this excited state as the fundamental in the methyl rotor. The next lowest energy state is obtained by requiring the wave function to change sign when the H_AH_B distance and the distance between H_B and H_C are equal. Motion along the H_AH_B/H_BH_C asymmetric stretch corresponds to motion across the C_{2v} saddle point, and we refer to this state as having excitation in the C_{2v} isomerization coordinate in the discussion that follows. The difference between the DMC and variational energies for this state is the largest of any of the energies reported in Table 4. We believe that this larger difference reflects the high sensitivity of the energy of this state to the reference geometry used for the VCI calculations. In particular, comparing the largest peak in the stick versions of the VCI spectra, reported in Figure 2b of ref 3, we find that the energy of this transition shifts by nearly 100 cm^{-1} between the calculations based on the C_s(I) and C_{2v} stationary points.[3]

For three of the remaining four excited states for which comparisons can be made, the agreement with the previously reported VCI results is excellent. The other excited state for which there is a notable difference between the energies that we obtain and those reported in ref 3 is the symmetric stretch involving the CH_D and CH_E bonds. While the reported VCI energy of this state is 84 cm^{-1} smaller than that for the CH_D/CH_E asymmetric stretch, our DMC results display the opposite trend with symmetric stretch having a frequency that is higher by 120 cm^{-1}. We believe that this difference reflects coupling between the CH stretch vibration and some of the lower frequency modes. When we analyze the wave functions associated with the two stretching states, we find that compared to the ground-state wave function, the asymmetric stretch has increased amplitude near the C_s(II) saddle point, while the symmetric stretch has more amplitude near the C_s(I) saddle point. Not surprisingly, the CH stretch frequencies fluctuate with methyl rotation and these symmetric and asymmetric CH stretch frequencies are higher at the minimum than at the C_s(II) saddle point.

4.3. Probability Distributions. While the energies are interesting and important, they can be obtained by other approaches. The power of DMC for studies of CH_5^+ comes in the fact that it provides a Monte Carlo sampling of the ground- and excited-state wave functions. We also evaluate the probability amplitudes using the descendent weighting approach.[33,35] The probability amplitudes allow us to obtain expectation values of any multiplicative operator of interest, along with projections of the probability amplitude onto any coordinate or pair of coordinates. Such information will be useful as we consider appropriate models for understanding the high-resolution spectra.[2,3] We will focus our discussion on four states, and briefly discuss the other calculated excited states. The states discussed in detail are the states with one quantum of excitation in the C_s and C_{2v} isomerization coordinates and the states with one quantum of excitation in the CH_A/CH_B and in the CH_D/CH_E asymmetric stretch coordinates.

We will discuss the excited states in terms of four projections of the probability amplitude. The first two involve the projection along the five CH and ten HH distances. These provide information about the overall size of the molecule. The remaining two distributions involve projections along the six methyl rotor coordinates $\phi_{\alpha,\beta}$, and the C_{2v} isomerization coordinate, q. As shown in Table 3, ϕ and q have different values at the four stationary points and the distributions that

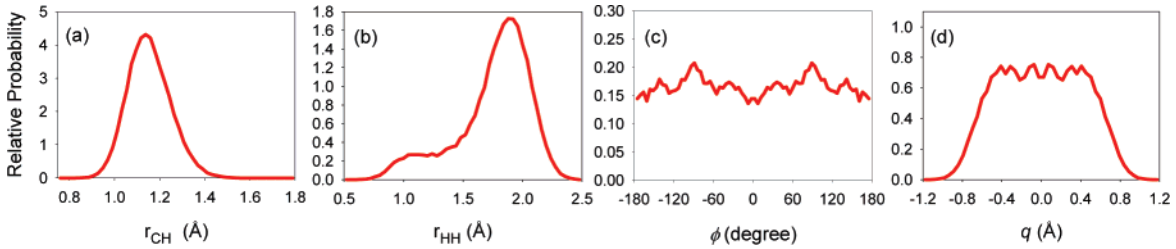

Figure 2. Probability distribution for the ground state of CH_5^+, projected onto (a) the CH distance, (b) the HH distance, (c) the methyl rotor coordinate, ϕ, and (d) the C_{2v} isomerization coordinate, q.

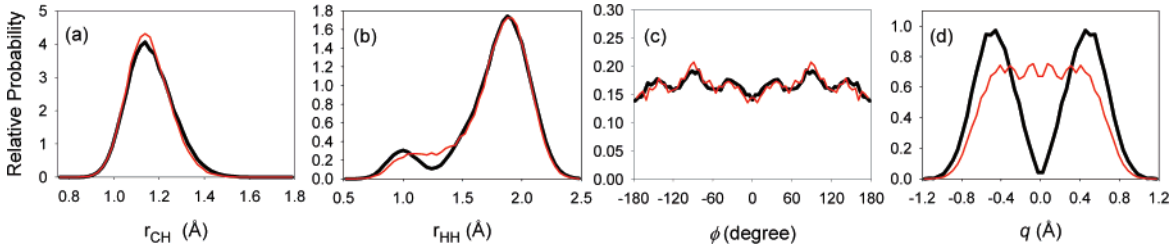

Figure 3. Same as Figure 2, with the projections of the probability amplitudes for the H_AH_B/H_BH_C asymmetric stretching fundamental plotted with thick black lines. The thin red lines provide the corresponding projections of the ground-state probability amplitude.

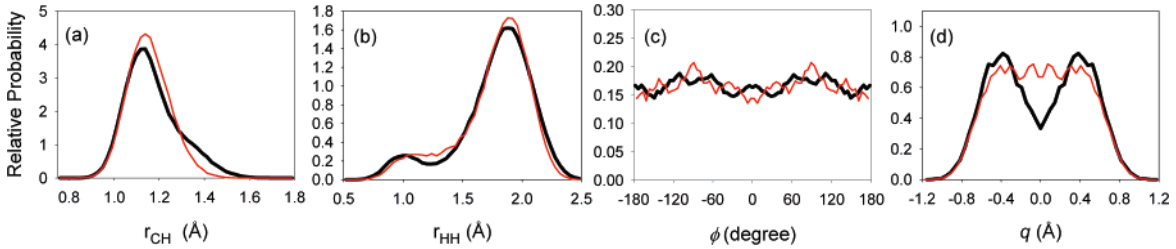

Figure 4. Same as Figure 2, with the projections of the probability amplitudes for the CH_A/CH_B asymmetric stretching fundamental plotted with thick black lines. The thin red lines provide the corresponding projections of the ground-state probability amplitude.

are plotted as functions of these coordinates provide information about the extent of localization of the wave function. In cases like the CH distance distribution, where there are five possible distances, the reported probability distribution reflects the sum of these distributions. This is done in order to ensure that the plotted distributions reflect the full permutational symmetry of CH_5^+.

The ground-state probability distributions have been explored in detail elsewhere.[14,16,17] They are presented in Figure 2 for purposes of comparison to the excited-state distributions. The CH bond length distribution, plotted in Figure 2a, has a full width half-maximum of approximately 0.23 Å. Based on the harmonic force constants for methane, this CH_5^+ distribution is roughly 25% wider than the CH distance distribution in CH_4.[36] The increased width of the CH distance distribution reflects the fact that the CH bond lengths, reported in Table 1, range from 1.08 to 1.20 Å whereas in methane they are all 1.09 Å. In addition, some of the harmonic CH stretch frequencies in CH_5^+ are considerably lower than those in methane.[8,37]

The HH distance distribution, shown in Figure 2b, has a large peak at 1.8 Å and a shoulder at 1 Å. The shoulder reflects the 0.95 Å separation of the hydrogen atoms labeled A and B at the two stationary points with C_s symmetry. The peak near 1.8 Å has contributions from the other nine hydrogen−hydrogen interatomic distances.

The remaining two distributions show the probability amplitude as functions of the two isomerization coordinates. The methyl rotor distribution, plotted in Figure 2c, has nearly equal amplitude at all values of ϕ. When the ground-state probability amplitude is projected onto the C_{2v} isomerization coordinate, shown in Figure 2d, it has approximately equal amplitude at $q = \pm 0.48$ Å and $q = 0$. These values of q correspond to the C_s(I) minimum and the C_{2v} saddle point structures of CH_5^+. In previous discussions of these distribution, we concluded that the ground-state wave function is delocalized among the 120 equivalent minima and has at least as much amplitude at the 180 saddle points characterized as C_s(II) or C_{2v} that separate these minima.[3,14]

By looking at changes in the distributions, described above, we can learn about the nature of the couplings in the excited-state wave functions. We focus the following discussion on four excited states. These excited states are obtained by requiring the wave function to change sign when two of the HH distances are equal, $r_{H_AH_B} - r_{H_BH_C} = 0$, $r_{CH_A} - r_{CH_B} = 0$, and $r_{CH_D} - r_{CH_E} = 0$, respectively.

We first consider the lowest energy excited-state calculated in this study. For this state we require the wave function to change sign when two of the hydrogen/hydrogen distances are equal. If we compare the probability distributions for this state to those from the ground state, we see little difference and consequently have not included plots of these distributions. This is not surprising for the fundamental in the methyl rotor coordinate. Specifically, comparing the range of CH and HH distances reported for the two stationary points with C_s symmetry in Tables 1 and 2, the differences are small. In addition, the methyl rotor distribution reflects an average over the six HCHH torsion angles and this averaging obscures the nodes in the excited-state wave function.

The next lowest energy excited-state considered in this study is the H_AH_B/H_BH_C asymmetric stretch fundamental, which has an energy of 271 cm^{-1}. The probability distributions for this excited state are plotted with black lines in Figure 3 while the corresponding ground-state distributions are plotted with thin red lines. Since the nodal surface is defined as $r_{H_AH_B} - r_{H_BH_C} = 0$, the distribution, plotted as a function of q in Figure 3d, goes to zero at $q = 0$ as expected. When the probability amplitude is projected onto ϕ and plotted in Figure 3c, the distribution exhibits a slight decrease in amplitude near $\phi = 90°$, compared to the corresponding ground-state distribution. This reflects the fact that when a node is placed at $q = 0$, or at the C_{2v} saddle points in the potential, the probability amplitude will decrease at these configurations and consequently increase near the other stationary points.

Comparing the two bond length distributions to the ground-state ones, we find that the CH distance distribution is slightly broadened, with increased probability at the longer CH distances. The HH distance distribution has a more distinct bimodal structure than is seen in the ground-state distribution. This further supports the observation that there is increased amplitude near the two stationary points with C_s symmetry and, consequently, a greater separation of the hydrogen atoms into a H_2 and a CH_3^+ subunit.

Next, we consider the fundamental in the CH_A/CH_B asymmetric stretch. This transition has an energy of 2432 cm^{-1}, which

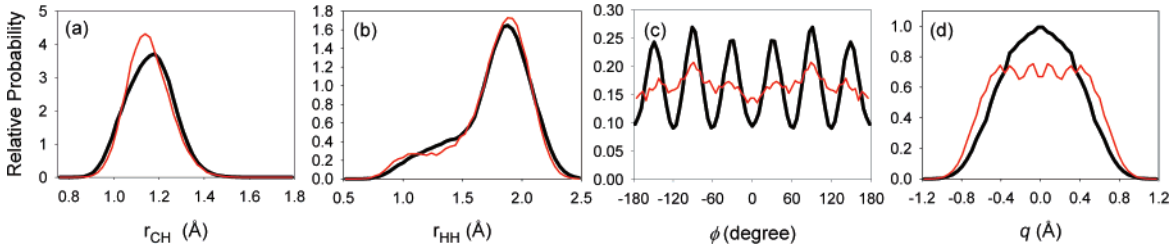

Figure 5. Same as Figure 2, with the projections of the probability amplitudes for the CH_D/CH_E asymmetric stretching fundamental plotted with thick black lines. The thin red lines provide the corresponding projections of the ground-state probability amplitude.

is in good agreement with the frequency at which there is a shoulder on the red side of the CH stretch band in the LIR spectrum.[4] The corresponding probability distributions are plotted in Figure 4. Here, the CH distance distribution shows increased probability amplitude at longer CH bond lengths. This reflects the nature of the excited state where we have required that one of the two longest CH distances be longer than another one. The HH interatomic distance distribution again shows a distinct H_2 group although it is not quite as pronounced as was seen in Figure 3. When the probability amplitude is projected onto ϕ and q, the resulting distributions resemble those which are obtained when a node is placed in the C_{2v} isomerization coordinate. When projected onto ϕ, the probability amplitude is approximately as delocalized as the ground states, but the small oscillations observed in the two plots are out of phase.

Another excited state of experimental interest is the fundamental in the CH_D/CH_E asymmetric stretch. This is most likely the state that has been accessed in the high-resolution studies,[2,3] and the calculated energy of 3023 ± 5 cm^{-1} is in good agreement with the accumulations of transitions near 3020 cm^{-1} in the 10 cm^{-1} convolution of the spectrum from obtained by Nesbitt and co-workers, plotted in Figure 3B of ref 3. The projections of the probability amplitude for this state are plotted in Figure 5. As with the CH_A/CH_B asymmetric stretch fundamental, plotted in Figure 4, the CH and HH distance distributions are broader than those for the ground state. In contrast to the three other states we have discussed, the hydrogen/hydrogen distance distribution does not show as pronounced a shoulder near 1 Å as it does in the ground state. In addition, the projection of the probability amplitude onto ϕ shows more structure than we saw in the other three plots of this distribution. This indicates that when we excite CH_5^+ along this asymmetric CH stretch, the molecule becomes partially locked into the C_s(II) configuration, shown in Figure 1b. At the C_s(II) geometry, the value of the C_{2v} isomerization coordinate is smaller than at the equilibrium geometry. Consequently, when the probability amplitude is projected onto q, the distribution is found to be narrower than the corresponding ground-state distribution. The changes in the distributions plotted in Figure 5c,d upon vibrational excitation reflect coupling between this stretching vibration, and, in particular, motion of the methyl rotor. As is well-know for systems that contain an internal rotor, coupling between the internal rotation and the end-over-end rotation of the molecule leads to rich rotational structure, especially when the height of the effective barrier to methyl rotation changes upon vibrational excitation.[38−41]

The probability amplitude for the other four excited states for which we report energies in Table 4 have also been studied. Based on the energies and analysis of the probability amplitudes, we find that the two states with energies near 1000 cm^{-1} correspond to bending modes. This is consistent with earlier assignments of the band in the LIR spectrum near 1100 cm^{-1} to HCH bends.[3,4] The excited-state that has an energy of 990 cm^{-1} is an HCH bend involving the methyl rotor group. When we analyze of the probability amplitude for this state, we find that the projections of the probability distribution onto ϕ and q resemble those for the CH_D/CH_E asymmetric stretch, shown in Figure 5. The second bend, at 1128 cm^{-1}, shows even greater localization in the projection of the probability amplitude onto ϕ, while the projection onto q resembles that of the ground state.

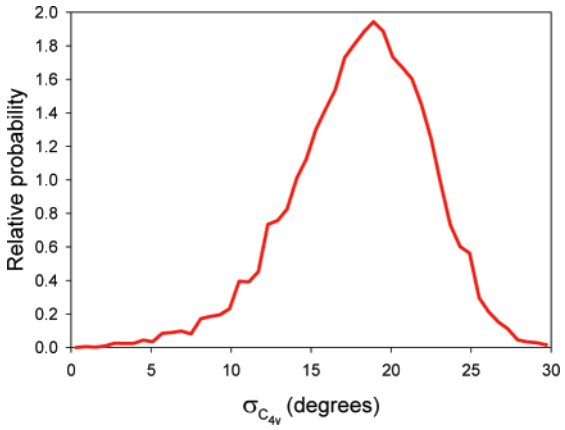

Figure 6. Projection of the ground-state probability amplitude onto $\sigma_{C_{4v}}$.

The remaining two states are the two CH symmetric stretches. The projections of the probability amplitude for the CH_A/CH_C symmetric stretch onto ϕ and q are nearly identical to those for the ground state, while the CH distance distribution is slightly broadened, as expected. Finally, as mentioned above, the distribution for the CH_D/CH_E symmetric stretch has more amplitude near the C_s(I) minimum energy structure, compared to the ground state, and, when the probability amplitude is projected onto q, the resulting distribution is slightly narrower than the corresponding ground-state distribution. When the probability amplitude is projected onto r_{CH} and r_{HH}, the distributions are both found to be broader than in the ground state.

4.4. C_{4v} Saddle Point. The discussion above has focused on the probability amplitude at the three lowest energy stationary points. As we discussed in section 2, there are other low-energy stationary points. In particular, the lowest energy configuration with C_{4v} symmetry has an energy that is only 1180 cm^{-1} above the global minimum. With a zero-point energy exceeding 10 900 cm^{-1}, one might expect that there would also be probability amplitude near this stationary point. We characterize the amount of probability amplitude near the C_{4v} structure by projecting the probability amplitude onto $\sigma_{C_{4v}}$, defined in section 2. This projection is plotted for the ground state in Figure 6. In this case, there is essentially no probability near the C_{4v} configuration. To quantify how the probability amplitude near this stationary point is affected by vibrational excitation, we report in the right column of Table 4 the fraction of C_{4v} character. This is defined as the fraction of the probability amplitude for

which $\sigma_{C_{4v}} < 2.5°$. The choice of 2.5° is somewhat arbitrary, but the general trends are the same if we use 1.0°, 2.5° or 5.0°.

Of the states we have investigated, two show a significant increase in probability amplitude near $\sigma_{C_{4v}}$. These are the CH_D/CH_E asymmetric stretch and the HCH bend within the methyl rotor group. Interestingly, these are the two states that have very similar projections of the probability amplitude onto q and ϕ. In particular, they display increased probability amplitude near the C_s(II) configuration, which is the stationary point that the C_{4v} structure of the molecule will relax toward.

5. Conclusions

Using fixed-node diffusion Monte Carlo techniques, we investigate the nature of the couplings in vibrationally excited states in CH_5^+. By requiring that the excitation remains localized in a single vibrational mode, we obtain good agreement between the energies calculated in this study and those previously reported VCI energies.[3] Interestingly, as we excite the molecule along the various CH stretch modes, we find substantial changes in the projections of the probability amplitude along the two isomerization coordinates, the methyl rotor coordinate, ϕ and the H_AH_B/H_BH_C asymmetric stretch. Increased structure in the distributions, when they are projected onto ϕ, indicate that the motion being considered leads to an increase in the effective barrier to methyl rotation. This is seen in the projections of the probability amplitude for the fundamental in the CH_D/CH_E asymmetric stretch, shown in Figure 5. Based on earlier VCI studies as well as harmonic frequencies and intensities, this is the state that provides the oscillator strength in the 3000 cm^{-1} region of the spectrum. It is hoped that this observation of significant coupling between the methyl rotor and this vibration will assist in the assignment of the high-resolution spectra that have been reported in this wave number region.[2,3]

In addition, we investigate the extent to which the C_{4v} saddle point is accessed in the various states that are investigated in this study. When the wave functions are analyzed, it is found that in those states, like the CH_D/CH_E asymmetric stretch, where there is increased probability amplitude near the C_s(II) saddle point compared to the ground state, there is also an increase in the amplitude near the C_{4v} saddle point.

Acknowledgment. Support through grants from the Chemistry Division of the National Science Foundation is gratefully acknowledged. We also thank Professor Joel M. Bowman for many discussions on these systems and for providing us with the codes used to evaluate the potential used in this work.

References and Notes

(1) Herbst, E. *J. Phys. Chem. A* **2005**, *109*, 4017.
(2) White, E. T.; Tang, J.; Oka, T. *Science* **1999**, *284*, 135.
(3) Huang, X.; McCoy, A. B.; Bowman, J. M.; Johnson, L. M.; Savage, C.; Dong, F.; Nesbitt, D. *J. Science* **2006**, *311*, 60.
(4) Asvany, O.; Kumar, P.; Redlich, B.; Hegeman, I.; Schlemmer, S.; Marx, D. *Science* **2005**, *309*, 1219.
(5) Nesbitt, D. J. Private communication.
(6) Schreiner, P. R.; Kim, S. J.; Schaefer, H. F. I.; Schleyer, P. v. R. *J. Chem. Phys.* **1993**, *99*, 3716.
(7) Muller, H.; Kutzelnigg, W.; Noga, J.; Klopper, W. *J. Chem. Phys.* **1997**, *106*, 1863.
(8) Jin, Z.; Braams, B. J.; Bowman, J. M. *J. Phys. Chem. A* **2006**, *110*, 1569.
(9) McCoy, A. B. *Int. Rev. Phys. Chem.* **2006**, *25*, 77.
(10) Brown, A.; Braams, B. J.; Christoffel, K.; Jin, Z.; Bowman, J. M. *J. Chem. Phys.* **2003**, *119*, 8790.
(11) Kumar, P. P.; Marx, D. *Phys. Chem. Chem. Phys.* **2006**, *8* (5), 573.
(12) Marx, D.; Parrinello, M. *Nature* **1995**, *375*, 216.
(13) Marx, D.; Parrinello, M. *Science* **1999**, *284*, 59, 61.
(14) McCoy, A. B.; Brown, A.; Braams, B. J.; Huang, X.; Jin, Z.; Bowman, J. M. *J. Phys. Chem. A* **2004**, *108*, 4991.
(15) Brown, A.; McCoy, A. B.; Braams, B. J.; Jin, Z.; Bowman, J. M. *J. Chem.* Phys. **2004**, *121*, 4105.
(16) Thompson, K. C.; Crittenden, D. L.; Jordan, M. J. T. *J. Am. Chem. Soc.* **2005**, *127*, 4954.
(17) Johnson, L. M.; McCoy, A. B. *J. Phys. Chem. A* **2006**, *110*, 8213.
(18) Hinkle, C. E.; McCoy, A. B.; Huang, X.; Bowman, J. M. *J. Phys. Chem. A* **2007**, *111*, 2033.
(19) Wang, X.-G.; Carrington, T. Private communication.
(20) Deskevich, M. P.; McCoy, A. B.; Hutson, J. M.; Nesbitt, J. M. *J. Chem. Phys.*, in press.
(21) Okulik, N. B.; Peruchena, N. M.; Jubert, A. H. *J. Phys. Chem. A* **2006**, *110*, 9974.
(22) Fleming, F. P.; Barbosa, A. G. H.; Esteves, P. M. *J. Phys. Chem. A* **2006**, *110*, 11903
(23) Tian, S. X.; Yang, J. L. *J. Phys. Chem. A* **2007**, *111*, 415.
(24) Huang, X.; Johnson, L. M.; Bowman, J. M.; McCoy, A. B. *J. Am. Chem. Soc.* **2006**, *128*, 3478.
(25) Anderson, J. B. *J. Chem. Phys.* **1975**, *63*, 1499.
(26) Anderson, J. B. *J. Chem. Phys.* **1976**, *65*, 4121.
(27) Lee, H.-S.; McCoy, A. B. *J. Chem. Phys.* **2002**, *116*, 9677.
(28) McCoy, A. B.; Huang, X.; Carter, S.; Bowman, J. M. *J. Chem. Phys.* **2005**, *123*, 064317.
(29) McCoy, A. B.; Huang, X.; Carter, S.; Landeweer, M. Y.; Bowman, J. M. *J. Chem. Phys.* **2005**, *122*, 061101.
(30) Hammer, N. I.; Diken, E. G.; Roscioli, J. R.; Myshakin, E. M.; Jordan, K. D.; McCoy, A. B.; Huang, X.; Carter, S.; Bowman, J. M.; Johnson, M. A. *J. Chem. Phys.* **2005**, *123*, 044308.
(31) McCunn, L. R.; Roscioli, J. R.; Johnson, M. A.; McCoy, A. B. *J. Phys. Chem. B* **2008**, *112*, 321−327.
(32) Lee, H.-S.; Herbert, J. M.; McCoy, A. B. *J. Chem. Phys.* **1999**, *110*, 5481.
(33) Suhm, M. A.; Watts, R. O. *Phys. Rep.* **1991**, *204*, 293.
(34) Bowman, J. M.; Carter, S.; Huang, X. *Int. Rev. Phys. Chem.* **2003**, *22*, 533.
(35) Langfelder, P.; Rothstein, S. M.; Vrbik, J. *J. Chem. Phys.* **1997**, *107* (20), 8526.
(36) Wang, X.-G.; Sibert, E. L. *J. Chem. Phys.* **1999**, *111*, 4510.
(37) Schuder, M. D.; Lovejoy, C. M.; Lascola, R.; Nesbitt, D. J. *J. Chem. Phys.* **1993**, *99*, 4346.
(38) East, A. L. L.; Kolbuszewski, M.; Bunker, P. R. *J. Phys. Chem. A* **1997**, *101*, 6746.
(39) Bunker, P. R.; Ostojic, B.; Yurchenko, S. *J. Mol. Struct.* **2004**, *695*, 253.
(40) Hougen, J. T.; Kleiner, I.; Godefroid, M. *J. Mol. Spectrosc.* **1994**, *163*, 559.
(41) Just, G. M. P.; McCoy, A. B.; Miller, T. A. *J. Chem. Phys.* **2007**, *127*, 044310.